RSC Advances

ROYAL SOCIETY OF CHEMISTRY

www.rsc.org/advances

Influence of carbon nanofillers on the curing kinetics of Epoxy-Amine Resin

L. Vertuccio[1]*, S. Russo[2], M. Raimondo[1], K. Lafdi[3], L. Guadagno[1]

[1]*Department of Industrial Engineering – DIIn – University of Salerno*
Via Giovanni Paolo II, 132 - 84084 Fisciano (SA), Italy

[2]*ALENIA Aeronautica SpA, Viale dell'Aeronautica, 80038 Pomigliano D'Arco (NA), Italy*

[3]*University of Dayton, 300 College Park Dayton Ohio 45440 USA*

**Corresponding author, e-mail: lvertuccio@unisa.it*

Phone: +39 089 964019

Abstract

The cure kinetic of an epoxy resin based on the tetrafunctional epoxy precursor N,N′-tetraglycidyl methylene dianiline-(TGMDA) hardened with 4,4-diaminodiphenyl sulfone (DDS) was investigated. The influence of carbon nanofillers (carbon nanotubes, carbon nanofibers, and graphene based nanoparticles) on the cure kinetic was studied. Kinetic analysis was performed by dynamic and isothermal differential scanning calorimetry (DSC). In dynamic experiments, the activation energy was computed by using an advanced iso-conversional method, while under the isothermal condition, the Kamal's model-diffusion controlled was applied to simulate the systems in the whole curing process. The isothermal analysis shows that the introduction of the diluent decreases particularly the activation energy of secondary amine-epoxy reaction. A similar effect was obtained by the dynamic DSC analysis that shows a decrease in the activation energy for $\alpha > 0.7$, value of conversion for which it is considered that the reaction of secondary amine is active. The inclusion in the resin of one-dimensional fillers does not lead to big differences in the curing kinetics behaviour with respect to the raw epoxy. An increase in the activation energy is found in the case of highly exfoliated graphite. It is likely due to a reduction of free molecular segments of the epoxy network entrapped inside self-assembly structures.

Keywords: *Polymer composites, Thermosetting resins, Thermal properties, Cure kinetics*

1. Introduction

Epoxy resin is widely used for carbon fiber-reinforced composites (CFRCs), due to its excellent processability and properties [1-3]. In the manufacturing of CFRCs based epoxy resins, the curing reactions are partially responsible of the adhesion between the matrix and fibers, and play a crucial role in determining the mechanical properties of the finished composite products. In order to meet high structural performance requirements for new CFRC applications, the performance of epoxy resin needs to be enhanced. For many applications, such as aerospace and aeronautics, the rapid development of nanoscience and technology offers the possibility to produce materials with properties that would be unattainable by traditional thermosetting resins. The use of carbon nanotubes (CNTs), graphitic carbon nanofibers (CNFs) and graphene-based nanoparticles as polymer reinforcements is a particularly attractive option to enhance the current polymer matrix properties. These nanofillers are used to enhance or provide physical properties, such as high storage moduli, suitable thermal expansion, thermal and electrical conductivity, and magnetic recording properties [4-6]. The addition of nanofillers can influence the interaction of the polymer matrix with fiber reinforcements and the resin curing process. The processing behaviour of neat polymer and their nanocomposites are significantly different. An understanding of the curing process of the nano-modified epoxy matrix can help to design and manufacture composite parts characterized by enhanced electrical and mechanical properties. Generally epoxy resins, obtained by solidifying the only epoxy precursor with hardeners for structural materials, are brittle and have poor resistance to crack propagation [7-8]. To overcome this drawback, the epoxy resins are mixed with modifying agents, such as low molecular weight polymers, reactive oligomeric compounds, plasticizers, reactive diluents, etc. which modify the viscosity of the resin so that the processability of the system is not impaired [9-13]. On the other hand, these components can strongly modify the curing kinetic. Kinetic analyses of pure epoxy resin carried out by differential scanning calorimetry (DSC) data have shown a wide range of activation energy values (28–158 kJ/mol) [14-15]. Although a variation in the activation energy for pure epoxy resin has been reported by many authors [14-15], this aspect of the curing kinetics is still a matter of debate, in fact several manuscripts have reported constant values in the activation energy during the curing reaction [16-17]. On the other hand, with the massive and rapid development of nanocomposites, different studies have also been aimed to understand the effects of carbon nanofillers on the curing kinetics of epoxy resins [18–28]. Very few efforts have been aimed to study the effect of (carbon nanostructured forms (CNTs, CNFs, graphene-based nanoparticles etc.)) on the curing reactions of the tetrafunctional epoxy resins. This type of epoxy precursor is of great scientific and industrial interest, especially in light of the very performing results already published on mixtures based on this precursor loaded with unidimensional and bidimensional carbon nanofillers. In particular, interesting values in the dc volume conductivity of the resin filled with CNTs and CNFs were found [29]. The electrical percolation threshold (EPT) for the

composite filled with CNTs and CNFs, falls in the range [0.1, 0.32] wt% and, beyond the EPT, the electrical conductivity can reach values higher than 1-2 S/m. Furthermore, low cost fillers, such as highly exfoliated graphite, might be more relevant and competitive to simultaneously impart electrical conductivity and strong mechanical reinforcement to the resin [30]. Graphene based nanoparticles, embedded in this tetrafunctional epoxy precursor, are also able to enhance adhesive properties [31]. Generally, after the selection of promising industrial formulations, the knowledge of aspects related to their curing kinetic is a fundamental requirement to optimize the manufacturing processes and therefore the properties of the final materials.

This paper is aimed to study the curing kinetics of very promising nanofilled epoxy systems recently developed. In particular, three types of nanofillers have been selected: a) CNTs, b) CNFs and c) carboxylated exfoliated graphite CpEG. These nanofillers have been chosen because are among the best performing filler to enhance the electrical properties of epoxy resins and CFRCs (high electrical conductivity and low EPT) [29,30,32,34,35]. Furthermore, the chosen nanofillers have proven to simultaneously enhance mechanical performance [30,-32,35]. A concentration by weight of 0.5 % of nanofiller was used because this amount is beyond the EPT and it is able to enhance all the analyzed properties [29-32].

The choice of the epoxy mixture determines the final properties of the cured resin especially in terms of mechanical and thermal properties. Generally, a tetrafunctional precursor assures good properties of the cured resin due to the high level of crosslinking density. The advantages of the use of DDS hardener is the high glass transition, the better chemical resistance and the thermal properties of the resulting network compared with aliphatic and cycloaliphatic amine-cured network. An epoxy precursor such as the TGMDA hardened with DDS is characterized by very good thermal and mechanical properties, but it is brittle and characterized by poor resistance to crack propagation. To overcome this drawback, this epoxy precursor was mixed with modifying agents, such as low molecular weight polymer reactive oligomeric compounds, plasticizers, fillers, reactive diluents, etc. which modify the viscosity of the resin so that the processability of the system is not impaired [15,37-38]. Diluents are used in the formulation to reduce the viscosity or/and to eliminate the need of solvents. They are grouped into two types: reactive diluents and non-reactive diluents. Reactive diluents are mono-epoxide compounds, which participate in the curing reaction and reduce the crosslinking density. However, the addition of diluent is generally associated with a reduction in mechanical strength, modulus and glass transition temperature (T_g). Therefore, the amount of diluent must be optimised by critically analyzing the thermo-mechanical properties while keeping the technical specification for a particular application in mind. In this paper the diglycidylether of 1,4 butanediol reactive diluent was select.

2. Experimental

2.1 Materials

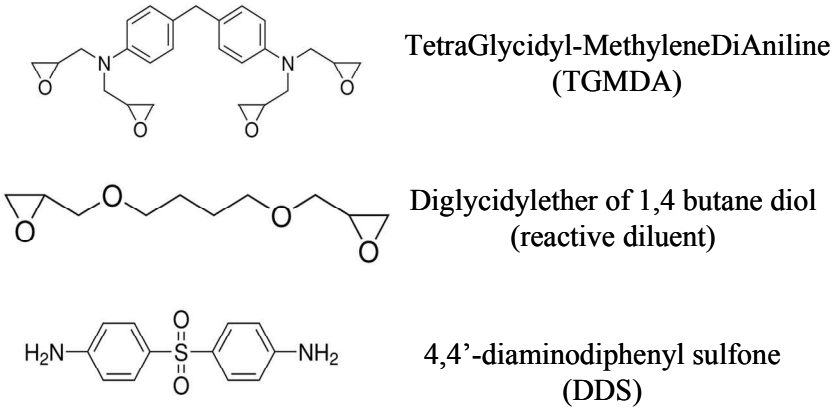

Fig. 1 Molecular structure of the chemical compounds.

Fig. 1 shows the chemical structures of the compounds used in this work. We have considered three types of fillers: carbon nanotubes and carbon nanofibers that have one dimensional (1D) predominant shape and highly exfoliated graphite that has a two dimensional (2D) predominant shape. The CNTs (3100 grade) were obtained from Nanocyl S.A. The specific surface area of multi-wall carbon nanotubes determined by using the BET method is around 250–300 m^2g^{-1}, the carbon purity is > 95 % with a metal oxide impurity < 5 % as it results by thermogravimetric analysis (TGA). A detailed analysis of the morphological parameters of the CNTs has been carried out by high resolution transmission electron microscopy (HR-TEM). Most of CNTs are characterized by an outer diameter ranging from 10 to 30 nm, but an outer diameter lower than 10 nm or larger than 80 nm has been also observed. Lengths of CNTs range from hundreds of nanometers to tens of micrometers. Number of walls varies from 4 to 20 in most nanotubes [39-40].

CNFs in the form of powders used in this study were produced at Applied Sciences Inc. and were from the Pyrograf III family. The CNFs were obtained by heat treatment at T=2500 °C starting from sample PR25XTPS1100 in order to provide the best combination of mechanical and electrical properties [32]. The heat treatment was performed in an atmosphere controlled batch furnace. Approximately 300 g of nanofibers were placed in a ceramic crucible for the heat treatment. The furnace was purged with nitrogen gas for 1 h prior to heating. The heating rate was 100 °C/h and the furnace was held at a temperature of 2500 °C for 1 h prior to cooling [32].

Previous papers highlighted that the heat treatment strongly influences the degree of structural ordering and therefore the bonding states of carbon atoms in the nanofiber structure [32]. It causes a significant transformation in the hybridization state of the bonded carbon atoms. The enhancement in

the fiber structural perfection very positively affects the electrical conductivity of the nanofiber-reinforced resins leading to an increase in the conductivity at very low filler concentration [32].

The sample CpEG was prepared as follows: a mixture containing nitric and sulphuric acid and natural graphite was used [31]. After 24 h of reaction, intercalation within graphene sheets took place to form intercalated graphite compound. Then the mixture was filtered, washed with water, and dried in an oven at low temperatures. The intercalated graphite compound was subjected to sudden heat treatment temperature of 900 °C and rapid expansion then occurred. The expansion ratio was as high as 300 times. The considered filler has a two dimensional (2D) predominant shape and it is obtained with an exfoliation procedure from natural graphite, that leads to obtain 2D conductive particles with an average diameter of 500 μm. The average value of Brunauer-Emmett-Teller specific surface area (S_{BET}) has been found to be 16.3 m^2g^{-1}.

2.2 Sample preparation

Five systems were prepared. In the first system, the epoxy precursor TGMDA was mixed with a stoichiometric amount of DDS, in an oil bath at 120 °C, (sample acronym TGMDA_DDS). The mixture was mechanically stirred until a homogeneous mixture was observed. In the second system, the epoxy matrix was obtained by mixing TGMDA with reactive diluent (diglycidylether of 1,4 butane diol) at a concentration of 80 %:20 % (by wt) epoxide to diluent.

The advantage of the used reactive diluent has been evidenced in previous work focused on the viscoelastic properties of CNF/epoxy resins. The inclusion of the reactive diluent diglycidylether of 1,4 butane diol in the epoxy resin based on the TGMDA precursor significantly reduces the viscosity values of the TGMDA, thus favouring the manufacturing process of the nanofilled resin [37-38]. Furthermore, the presence of oxirane rings in the reactive diluent allows efficient crosslinking reactions with the chains of the diluent included in the epoxy network.

DDS was added at a stoichiometric concentration with respect to all epoxy rings (sample acronym TGMDA_DDS_DILUENT). In the nanofilled resins corresponding to the last three systems, CNTs, CNFs and CpEG were embedded at loading rate of 0.5% by weight in the epoxy mixture TGMDA-DDS-DILUENT by using ultrasonication for 20 minutes (Hielscher model UP200S- 24 kHz high power ultrasonic probe). These nanocomposites (based on TGMDA_DDS_DILUENT epoxy mixture) are named respectively as follows: CNTs system, CNFs system, CpEG system.

2.3 Methods: Differential Scanning Calorimeter (DSC) and Scanning Electron Microscopy (SEM)

The DSC instrument measures heat flow into or from a sample under heating, cooling or isothermal conditions. DSC measures the quantitative heat flow as a direct function of time or of the sample temperature. This heat flow temperature data provides extremely valuable information on key physical and chemical properties associated with thermosetting materials, including: glass transition temperature (T_g), onset and end of cure, heat of curing, maximum rate of curing, percentage of curing, heat capacities. These properties can then be used to address some of the everyday problems, which confront the manufacturer, or user of thermosetting resins.

Differences between isothermal and dynamic curing kinetics have been an ongoing debate in the literature from the early days of kinetic modeling and commercial DSC's (1960's-70's), to recent literature reviews [41]. For purely kinetic studies, dynamic tests are still considered more reliable since their baselines, start and end points can be defined more easily. However, isothermal tests (or their residuals) are necessary for diffusion modeling. In general, cure models are not compared to both isothermal and dynamic data, although those pursuing advanced modeling programs assert that the two test modes should be used as complimentary data sources to cover the widest range of temperatures, degrees of cure, and material behaviour as possible [42-43].

A differential scanning calorimeter (Mettler DSC 822) was used for the dynamic and isothermal cure experiments and for data analysis under an nitrogen flow of 20 ml/min. To select suitable temperatures for the required isothermal experiments, a dynamic DSC scan at a heating rate of 10 °C/min was first obtained (see Fig. 2). Values of temperature above but near the onset of reaction were chosen. This method could avoid the improper choice of temperature, which may be too high or too low. Isothermal experiments were carried out at 180 °C, 190 °C, 200 °C, 210 °C, and 220 °C. The reaction was considered complete when the signal leveled off to baseline. The total area under the isotherm curve, based on the extrapolated baseline at the end of the reaction, was used to calculate the isothermal heat of reaction, $\Delta H_i(t)$ (i= 180 °C, 190 °C, 220 °C), at a given temperature (see Fig. 2). After each isothermal scan, the sample was rapidly cooled in the DSC cell to 30 °C and then reheated at 10 °C/min to 300 °C to determine the residual heat of reaction, $\Delta H_{residue}$ (see the inset of Fig. 3) .

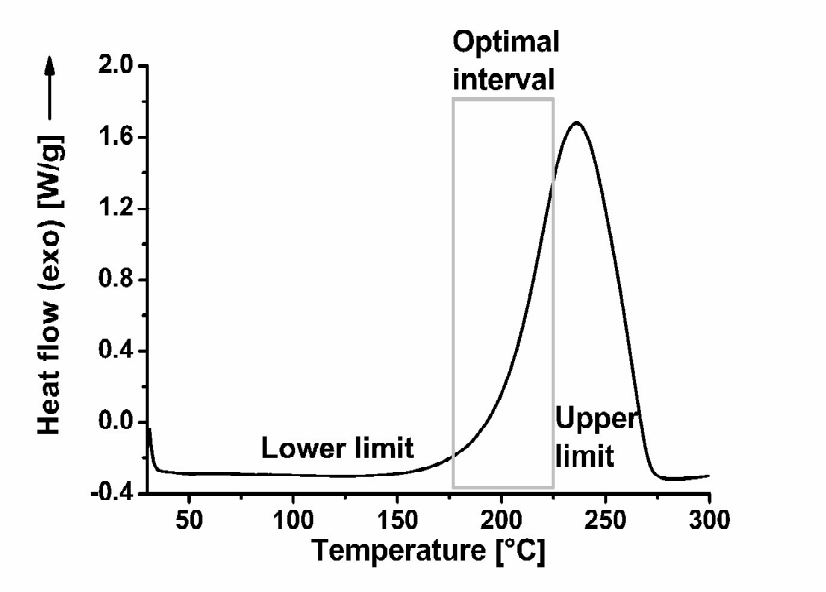

Fig. 2 Selection of isothermal curing temperature.

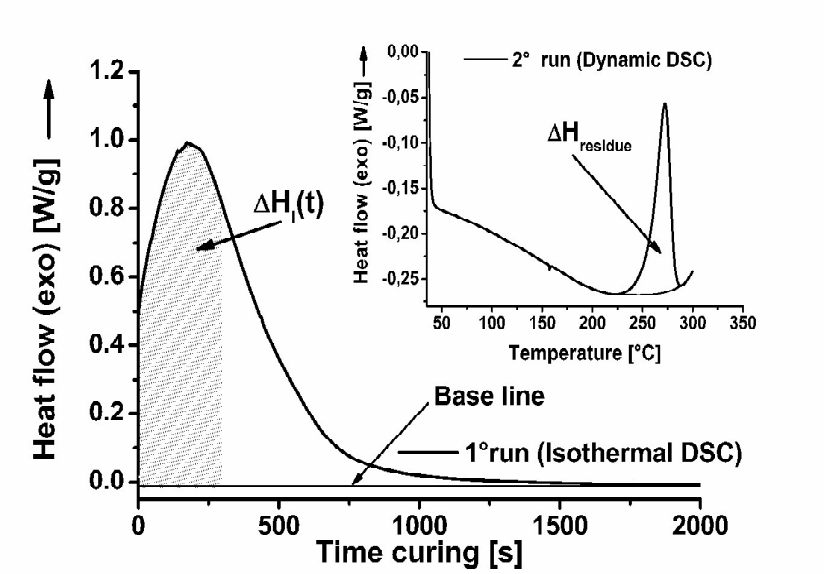

Fig. 3 A typical isothermal DSC curing curve.

The total heat evolved during the curing reaction is $\Delta H_{tot}=\Delta H_i+\Delta H_{residue}$ where ΔH_i is the total heat released during the cycle isothermal. The degree of cure, α, is related to the enthalpy released during the exothermic reaction of the resin components. The relation is given in Equation (1), where $\Delta H_i(t)$ is the partial heat of reaction at a certain time and ΔH_{tot} is the total heat of reaction.

$$\alpha(T,t)=\frac{1}{\Delta H_{tot}}\int_0^t\left(\frac{dH}{dt}\right)dt=\frac{\Delta H_i(t)}{\Delta H_{tot}} \quad (1)$$

The rate of reaction as a function of time has been calculated from the rate of heat flow measured in isothermal DSC experiments:

$$\frac{d\alpha}{dt} = \frac{dH/dt}{\Delta H_{tot}} \quad (2)$$

The dynamic cure experiments were performed at 2.5, 5, 10 and 20 °C / min from 30 to 300 °C.
Micrographs of the carbon nanofillers CNTs, CNFs and CpEG and their corresponding nanocomposites were obtained using a Scanning electron microscopy (SEM, mod. LEO 1525, Carl Zeiss SMT AG, Oberkochen, Germany). All the samples were placed on a carbon tab previously stuck to an aluminum stub (Agar Scientific, Stansted, UK) and were covered with a 250-A° -thick gold film using a sputter coater (Agar mod. 108 A). Nanofilled sample sections were cut from solid samples by a sledge microtome. These slices were etched before the observation by SEM. The etching reagent was prepared by stirring 1.0 g potassium permanganate in a solution mixture of 95 mL sulfuric acid (95 % - 97 %) and 48 mL orthophosphoric acid (85 %). The filled resins were immersed into the fresh etching reagent at room temperature and held under agitation for 36 h. Subsequent washings were done using a cold mixture of two parts by volume of concentrated sulfuric acid and seven parts of water. Afterward the samples were washed again with 30 % aqueous hydrogen peroxide to remove any manganese dioxide. The samples were finally washed with distilled water and kept under vacuum for 5 days before being subjected to morphological analysis.

3. Results and discussion

3.1. Morphological investigation

The inclusion in the resin of one-dimensional fillers does not lead to big differences in the curing kinetics behaviour with respect to the raw epoxy. An increase in the activation energy is found in the case of highly exfoliated graphite. It is likely due to a reduction of free molecular segments of the epoxy network. In order to fully understand the influence of carbon nanofillers (CNTs, CNFs, CpEG) on the curing kinetics of Epoxy-Amine Resin, the morphologies of both carbon nanoparticles and nanofilled systems were characterized. SEM investigation on the carbonaceous nanofillers was performed to analyze their morphological features before their incorporation into the epoxy precursors (see Fig. 4). The morphological features of CNTs are very different from the other unidimensional filler CNF. They tend to assemble due to the more intense van der Waals interactions between monofilaments characterized by lower value in the diameters with respect to the CNFs. In Fig. 4 we can observe that the CNFs are characterized by straighter walls where the nested configuration, typical of the as made CNFs, is not clearly visible, according to the previous results [32,37]. The heat treatment seems able to statistically reduce this effect. In fact after heat-treating the as made nanofibers to a

temperature of 2500°C, the graphene layers became straight, and the minimum interlayer spacing was reached for the nanofibers. Lengths of CNFs range from about 50 to 100 μm and the diameter of CNFs range from 125 to 150 nm. SEM image of the CpEG sample shows a fluffy morphology, characteristic of graphite subjected to heat treatment, where we can see few layers of large surface area highly wrinkled and folded.

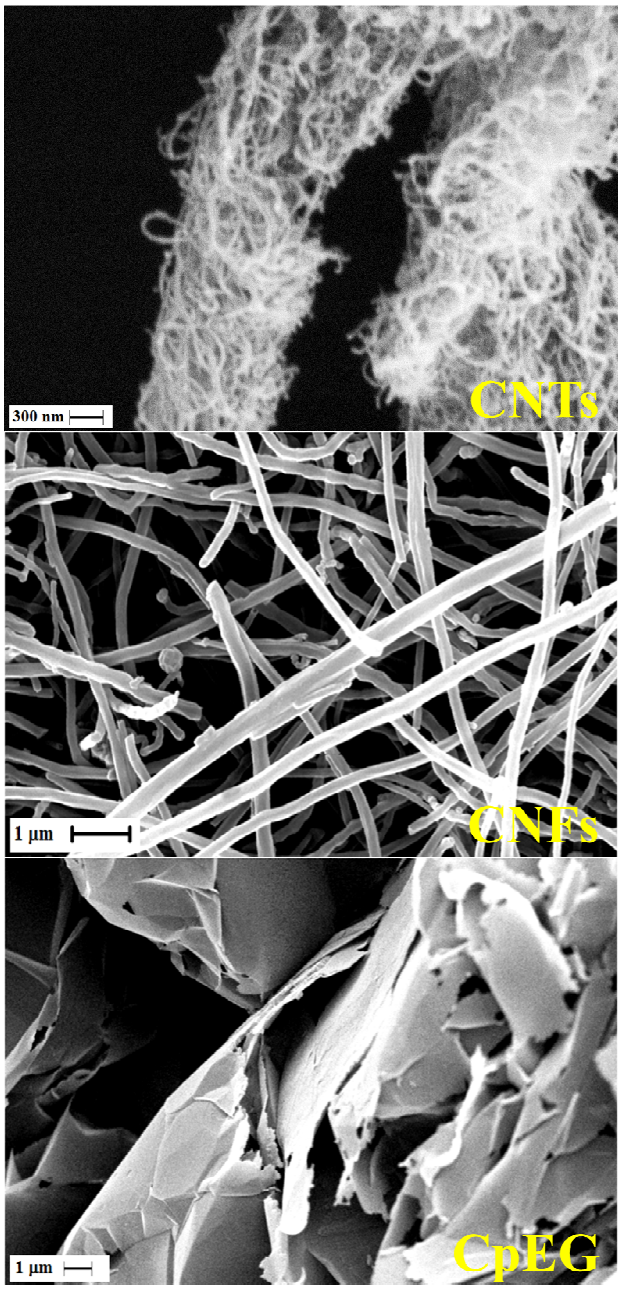

Fig. 4 SEM images of the three different carbonaceous nanofillers

The morphological feature of the nanofillers has proven to play a relevant role in determining the electrical and mechanical properties of the analyzed nano-filled resins [30-31]. The results on the electrical properties obtained for the composite with MWCNT and CNFs, above the percolation threshold, are among the highest values of electrical conductivity obtained for epoxy systems [30] . At low filler contents, the composite exhibits an electrical conductivity comparable to that of the pure polymer. Instead, near the percolation threshold which is different for the diverse systems, the composite exhibits a transition from an insulating to a conducting behaviour. For both composites, the percolation threshold is lower than 0.3% by weight. At higher filler concentrations the electrical conductivity reaches a plateau at a value several orders of magnitude above that of the neat resin.

Concerning the filler CpEG, a careful morphological investigation of the sample loaded with CpEG was already performed in literature [30]. The results for the composite with CpEG highlight the relevant influence of the exfoliation degree and the role of edge-carboxylated graphite layers to originate self-assembly structures embedded in the polymeric matrix [30]. Detailed analysis at nanoscale, carried out by means of Transmission Electron Microscopy (TEM) and Atomic Force Microscopy (AFM), highlighted that Graphene layers inside the epoxy matrix may serve as building blocks of complex systems that could outperform the host matrix [30]. Groups on EG responsible of the self-assembled structures were highlighted by elementary analysis (presence of functional groups containing C and O), FT/IR analysis and thermogravimetric investigation [30]. In particular, the CpEG sample highlighted self-assembly structures created by edge-carboxylated graphene layers or graphitic blocks which can provide superb polymer–CpEG interactions through intermolecular hydrogen bonding also with the polar groups of the resin network [30]. This strategy favors the interfacial interaction between polymer and carbon layer enhancing the electrical percolation paths and mechanical performance. An increase in the mechanical performance in terms of tensile strength and Young's modulus of thermoplastic nanocomposites, due to the effect of nanofiller (CNT) functionalization and hence the enhancement of the interfacial interaction, was already reported by other authors [44,45]

In order to analyze the homogeneity of the nanofiller dispersion in the polymeric matrix, morphological analysis by SEM was carried out on etched samples to remove the resin surrounding the nanofillers, leaving them bare. Fig. 5 shows SEM images of the fracture surface of the three epoxy-based composites filled with 0.5 wt% loading of nanofillers (CNTs system, CNFs system and CpEG system respectively). The used etching procedure, reported in the experimental, mainly consumes the surface layers of the polymeric matrix. We observe that the same etching procedure seems to be more efficient for composites filled with CNTs and CNFs. In fact, in this case we observe whole lengths of the CNTs and CNFs segments released from the residual resin fraction, highlighting a homogeneous structure for both the samples, in which the nanofillers are uniformly distributed in the epoxy matrix. The observation of the image in Fig. 5 shows that only a few layers of graphene appear bare and clearly visible in the surface, emerging from the resin. This can be explained assuming that strong interconnections between CpEG particles and residual polymeric matrix remain after the

etching attack. Edge-carboxylated graphene nanosheets by increasing the CpEG/epoxy matrix interaction favor a more efficient load transfer and consequently determine a strong mechanical reinforcement in the elastic modulus [30].

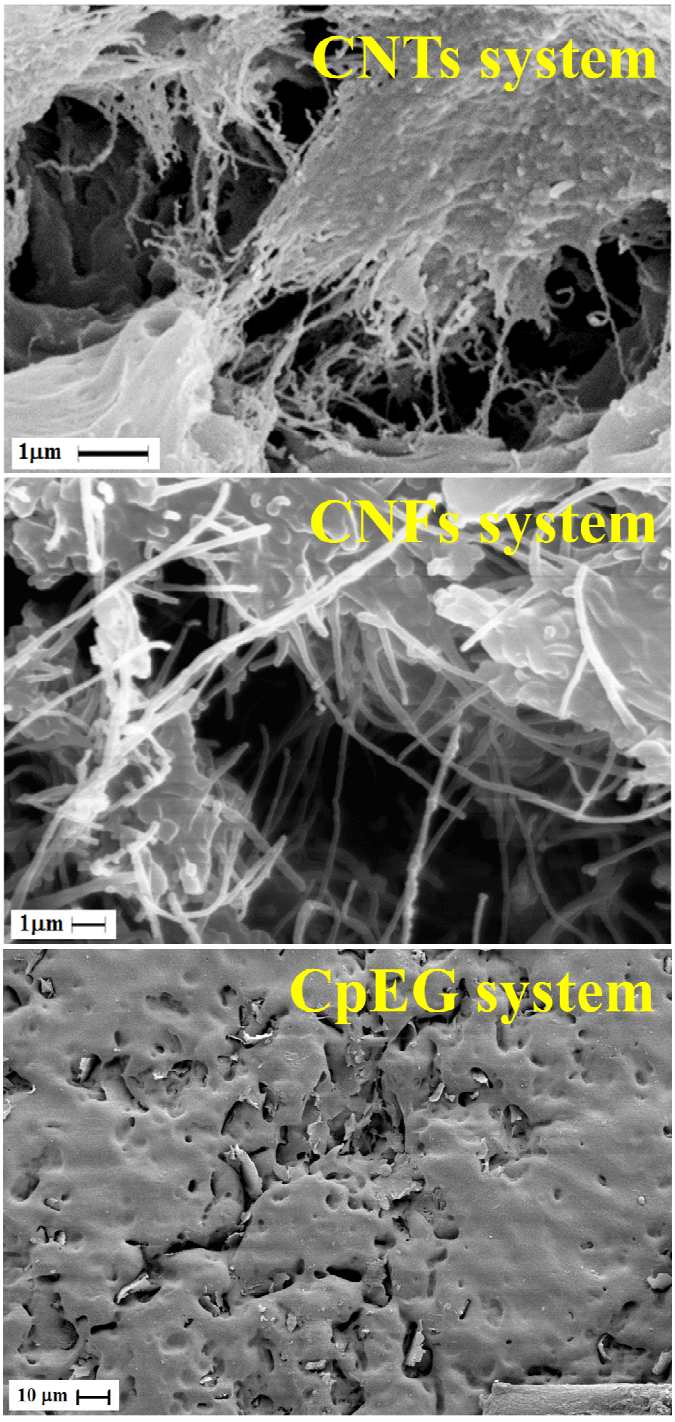

Fig. 5 SEM images of the fracture surface of the three different epoxy systems with 0.5 wt% loading of nanofillers

3.2 Curing behaviours (Isothermal DSC analysis)

A series of isothermal reaction rate curves for sample TGMDA_DDS (obtained from DSC measurements), as a function of time, is shown in Fig. 6.

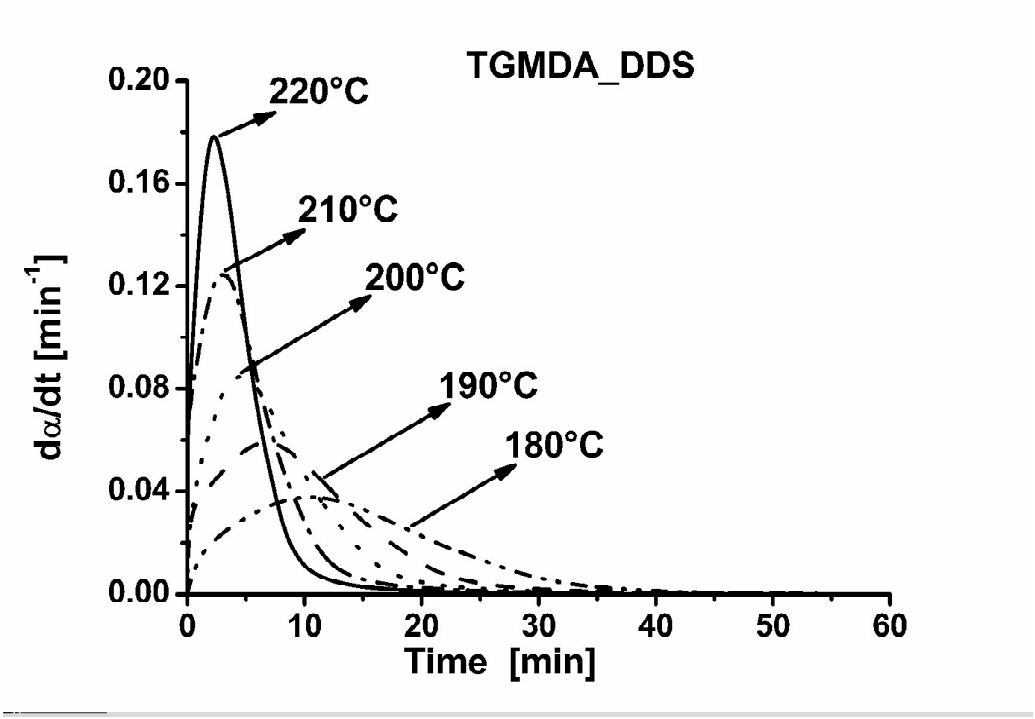

Fig. 6 Isothermal reaction rate as a function of time at different curing temperature for TGMDA_DDS.

The curve profiles highlight that the reaction rate increases rapidly because of the auto-acceleration and reaches a maximum. After this point it starts to decrease and gradually dies out. The increase in temperature of the curing reaction influences the value of the reaction rate at the maximum. The peak of the reaction rate becomes higher and shifts to a shorter time along with the increasing the curing temperature. The plot shows the maximum in the $d\alpha/dt$ versus time-curve at $t \neq 0$; which is characteristic for autocatalytic reactions [26,46]. By partial integration of areas under the experimental curves in Fig. 3, the fractional conversion as a function of time has been obtained.

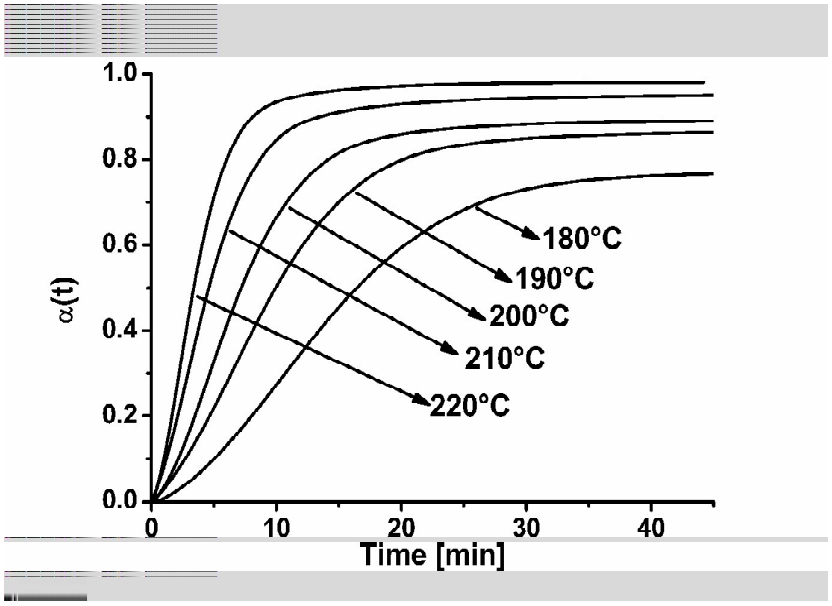

Fig. 7 Isothermal fractional conversion as a function of time at different curing temperature for TGMDA_DDS.

Fig. 7 presents the plot of curing reaction conversion (calculated from the experimental data) versus time at different isothermal temperatures. Initially, the conversion level increases with time and finally approaches a limiting conversion. The higher the curing temperatures the higher the limiting fractional conversion is reached. This is to be expected since in step of polymerisation the original monomer disappears early in the reaction and after the gel point most of reactive functional groups are attached to the cross-linked network. Different models have been proposed to describe the curing behaviour of thermoset resins. For amine-cured epoxy resins, it is generally accepted that two main addition reactions, described as primary and secondary-amine ring-opening, are occurring [47]. In this work Kamal's model (describing the chemically controlled cure), arising from the autocatalytic reaction mechanism is applied to our isothermal data. Kamal proposed the following expression [48]:

$$\frac{d\alpha}{dt} = \left(k_1 + k_2\alpha^m\right)(1-\alpha)^n \tag{3}$$

where m and n are the reaction orders, and k_1, k_2 are the rate parameters which are functions of temperature. Non-linear regression analysis is used for the computation of the parameters: m, n and k_2; while the reaction rate constant k_1 was determined as the initial reaction rate at t = 0, given by the intercept of curves of the reaction rate versus time. In order to incorporate the effects of diffusion on curing kinetics, several ways have been proposed. One way is to invoke the Rabinowitch concept [49], which defines the overall rate constants k_1 and k_2 in Eq. (3) as a function of the chemically controlled rate constant (k_c) and the diffusion term (k_d)

$$\frac{1}{k_i} = \frac{1}{k_c} + \frac{1}{k_d} \tag{4}$$

where i = 1 and 2. The diffusion term can assume either the modified WLF form [50] or modified Doolittle free volume form [51]. Another way of incorporating the effects of diffusion is to define a diffusion factor (f_d) [52] which equals to the ratio of the measured rate of reaction to the chemically controlled rate of reaction (i.e., in the absence of diffusion). Thus, the overall kinetic expression in form of Eq. (3) can be expressed as

$$\frac{d\alpha}{dt} = \left(k_1 + k_2\alpha^m\right)(1-\alpha)^n f_d(\alpha) \tag{5}$$

A commonly used expression for f_d, which was originally proposed by Chern and Poehlein [53], has the final form [54] of

$$f_d(\alpha) = \frac{1}{1+\exp\left[C(\alpha-\alpha_c)\right]} \tag{6}$$

where C and α_c are temperature-dependent fitting parameters. When α is much lower than the critical conversion α_c, $f_d(\alpha)$ approaches unity and the effects of diffusion are negligible. However, when α approaches α_c, $f_d(\alpha)$ decreases and eventually vanishes with further increase in conversion.

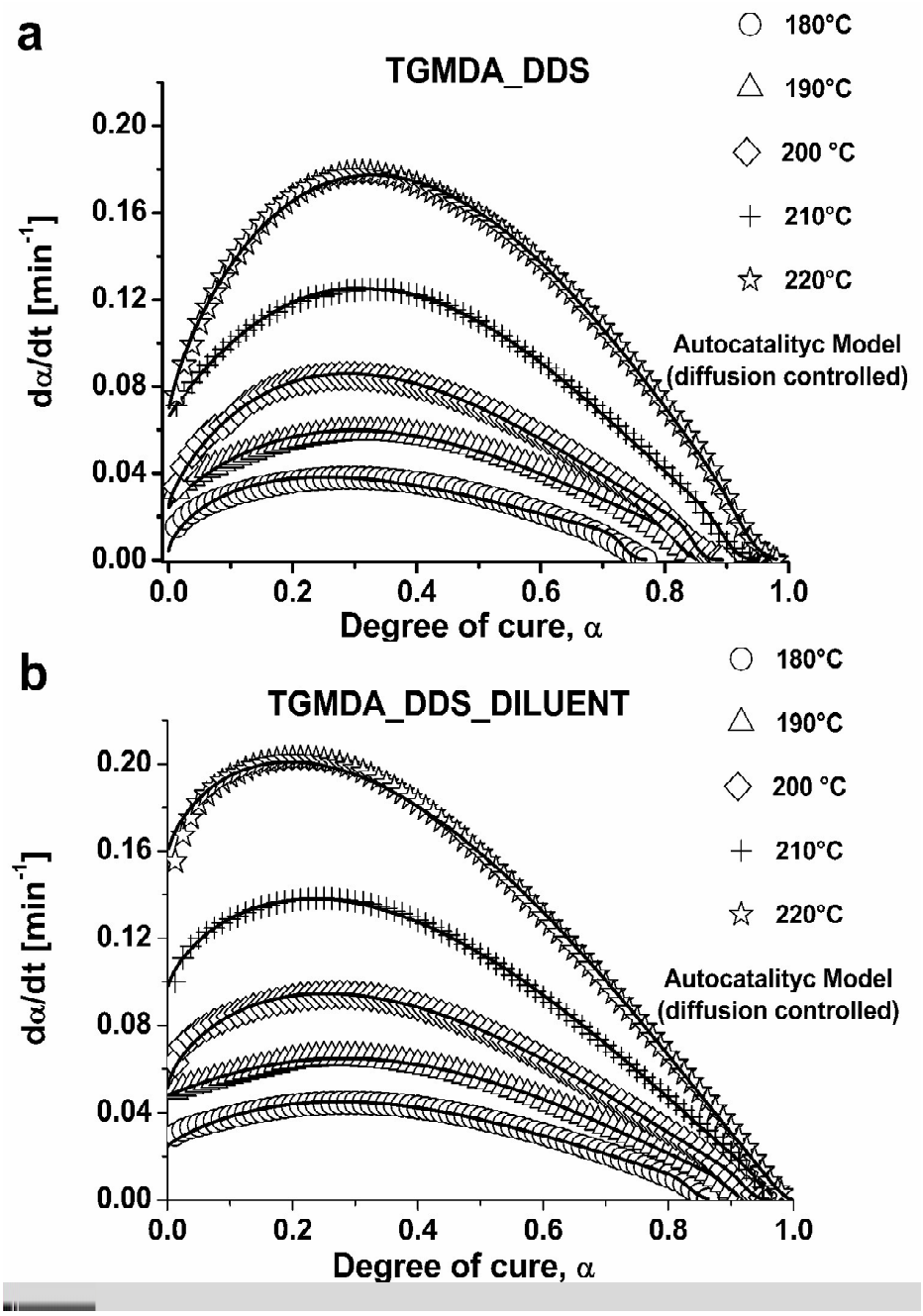

Fig. 8 Comparison of calculated data included the diffusion effect (solid line) with experimental data (symbols) for the system TGMDA_DDS a) and TGMDA_DDS_DILUENT b) respectively.

Table 1. Values of the kinetic parameters each sample obtained

T (°C)	k_1 [min^{-1}]	k_2 [min^{-1}]	n	m	m+n	α_c	α_{max}	E_1 [KJ/mol]	E_2 [KJ/mol]	ln A_1	ln A_2
	TGMDA_DDS										
180	0.0039	0.1456	1.78	0.64	2.42	0.734	0.770				
190	0.0244	0.2531	1.67	0.92	2.58	0.824	0.865				
200	0.0250	0.3361	1.63	0.80	2.43	0.848	0.893	125.73	60.35	28.32	14.20
210	0.0658	0.4707	1.48	0.97	2.45	0.903	0.952				
220	0.0680	0.5375	1.24	0.79	2.03	0.940	0.981				
	TGMDA_DDS_DILUENT										
180	0.0246	0.1543	1.56	0.88	2.43	0.837	0.864				
190	0.0480	0.2106	1.44	1.04	2.48	0.900	0.929				
200	0.0510	0.2223	1.28	0.69	1.96	0.927	0.960	81.84	34.21	18.04	7.24
210	0.0964	0.2794	1.22	0.74	1.96	0.960	0.987				
220	0.1578	0.3360	1.18	0.73	1.91	0.991	1.000				
	CpEG system										
180	0.0213	0.1292	1.42	0.76	2.17	0.861	0.888				
190	0.0434	0.1790	1.31	0.67	1.98	0.888	0.922				
200	0.0682	0.2060	1.34	0.76	2.10	0.902	0.942	79.46	49.33	17.40	11.04
210	0.1044	0.2726	1.21	0.79	2.00	0.963	0.988				
220	0.1152	0.3961	1.19	0.69	1.88	0.994	1.000				
	CNTs system										
180	0.0239	0.1529	1.55	0.81	2.36	0.855	0.882				
190	0.0445	0.1611	1.45	0.80	2.25	0.892	0.921				
200	0.0702	0.2063	1.30	0.80	2.11	0.924	0.958	85.89	39.99	19.13	8.65
210	0.1004	0.2867	1.24	0.79	2.03	0.970	0.989				
220	0.1602	0.3376	1.23	0.78	2.01	1.003	1.000				
	CNFs system										
180	0.0262	0.1558	1.56	0.94	2.50	0.865	0.890				
190	0.0346	0.1950	1.45	0.84	2.29	0.891	0.921				
200	0.0714	0.2132	1.29	0.86	2.14	0.940	0.970	84.30	41.82	18.66	9.21
210	0.0882	0.3202	1.27	0.86	2.13	0.973	0.991				
220	0.1588	0.3757	1.24	0.90	2.14	0.989	1.000				

The comparison, for the samples TGMDA_DDS and TGMDA_DDS_DILUENT, of the best fitted, to Eq. (5), curves with the corresponding experimental data is shown in Fig. 8.

Fig. 8 clearly shows that Eq. (5) leads to a very good description of the experimental data in the whole range of α. The kinetic parameters determined for the amine-cured TGMDA resin system are listed in Table 1 along with the correlation coefficient values for the curve fit. The maximum degree of cure α_{max} increased with higher temperatures. The critical degree of cure α_c increases with temperature. The reason for the decreasing effect of diffusion with higher temperature is that the thermal energy is high enough to maintain high molecular mobility to continue the cure [55]. The values of the reaction rate constants is between 0.039 min^{-1} and 0.680 min^{-1} for the primary and between 0.1456 min^{-1} and 0.5375 $min^{-1}$for the secondary reaction. The reaction rate constants k_1 and k_2 increase with the temperature. The temperature dependence of the rate constants is given by the Arrhenius expressions in Equation (7), where i indicates the primary or secondary amine-epoxy reaction, A_i is the pre-exponential factor, E_i the activation energy, R is the universal gas constant and T the reaction temperature.

$$k_i = A_i \exp^{\frac{-E_i}{RT}} \qquad i = 1,2 \tag{7}$$

Once the rate constants were identified, the activation energy E_i for both parts of the reaction and correlating pre-exponential factor A_i were derived from the slope and intercept of the plot $\ln(k_i)$ as a function of 1/T (1/K).(see Fig. 9)

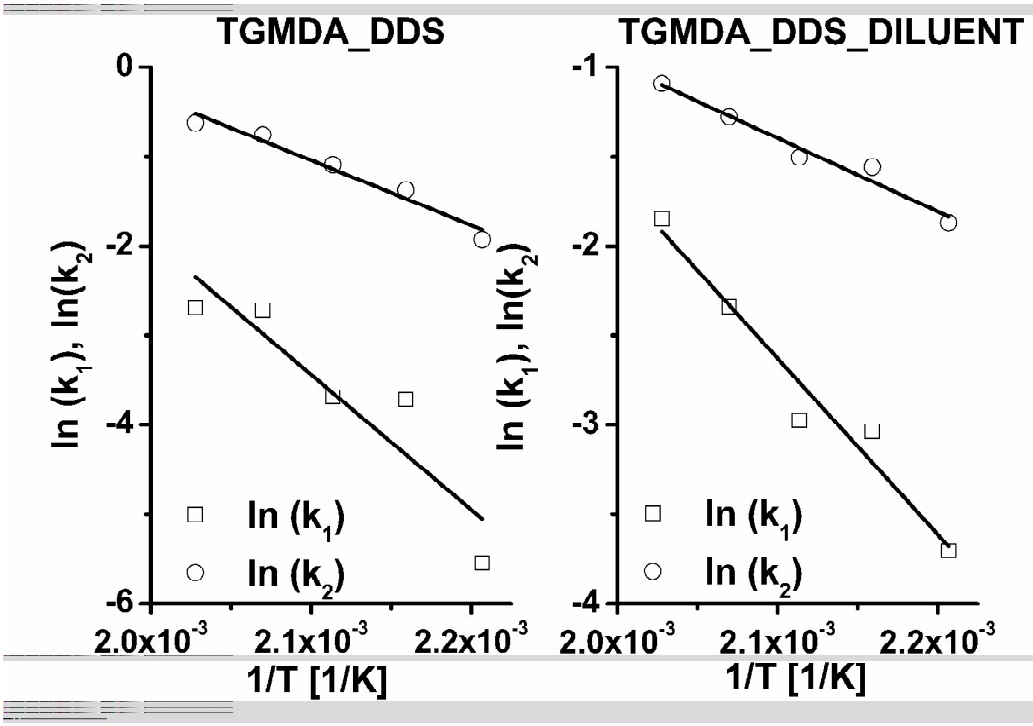

Fig. 9 Curve of ln (k_1) and ln (k_2) against 1/T for the samples TGMDA_DDS and TGMDA_DDS_DILUENT.

Table 1 shows the kinetic parameters obtained for the epoxy resin system with the reactive diluent by the isothermal DSC analysis. The activation energy E_1 and E_2 decreased significantly compared to the system without the reactive diluent. This means that the new epoxy system needs a lower amount of heat to curing. In particular E_2 decreases by about approximately 50 %, compared to the value obtained with the system TGMDA-DDS. The effect of the reactive diluent is remarkable for secondary amine-epoxy reaction. This result leads to consider the possibility of being able to cure the resin at lower temperatures. This consideration is evident in the Fig. 10 in which the profiles of isothermal heating at 220 °C for the two systems considered and the subsequent heating in dynamic mode are shown.

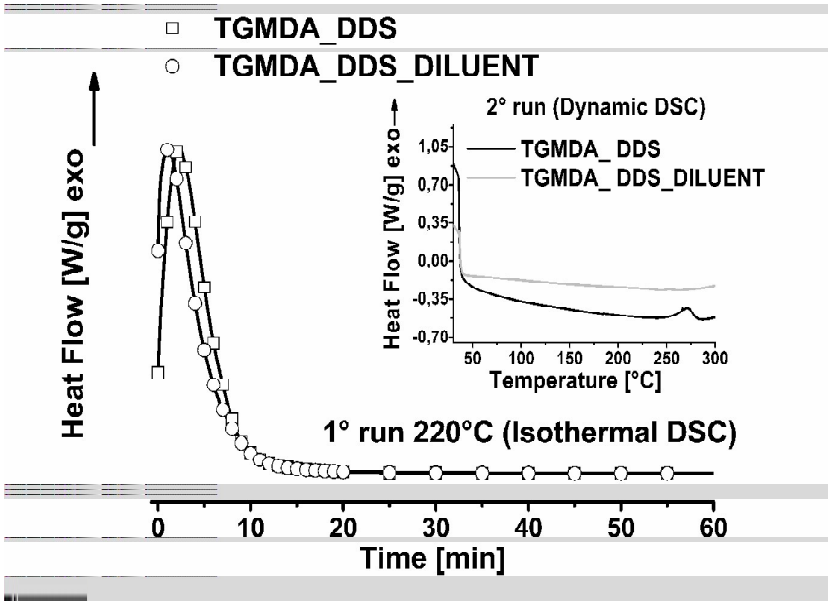

Fig. 10 Isothermal DSC curing curve for the system TGMDA_DDS and TGMDA_DDS_DILUENT.

The peak temperature decreases from a value of 134 seconds for the system TGMDA_DDS to 66 seconds for the system TGMDA_DDS_DILUENT, while the residual heat of reaction is absent for the epoxy system with the reactive diluent (see inset Fig. 10). This effect is more pronounced if the temperature of cure is lower, in fact the difference in maximum conversion (Table 1) obtained for both systems increases with the decrease of the temperature of cure as is evident in Fig. 11. This very interesting result highlights that a lower temperature of the curing process can be used in the formulation with the reactive diluent.

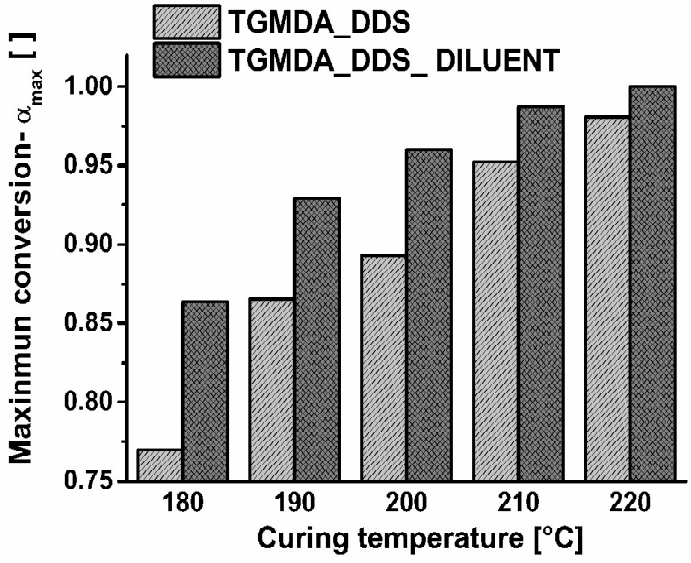

Fig. 11 The maximum degree of cure α_{max} vs curing temperature for the system TGMDA_DDS and TGMDA_DDS_DILUENT.

For systems loaded with different fillers, Table 1 shows that the value of E_1 and E_2 are similar to the values of the system with the diluent reactive except for the value E_2 obtained for the exfoliated graphite composite. It changes from 34 KJ/mol of the raw resin to 49 KJ/mol of the composite. E_2 is the activation energy for secondary amine-epoxy reaction when the viscosity is increased with the increase of the curing degree, thus more energy was required to overcome the motion among molecule chains. The obstacle opposed by exfoliated graphite decreases the free movement of molecules of the epoxy resin which translates to an increase of E_2

3.3 Dynamic DSC analysis (Iso-conversional methods and model-free kinetics)

If changes in the mechanism are associated with changes in the activation energy, they can be detected by using the model-free iso-conversional methods [56-61]. These methods are based on the iso-conversional principle that states that the reaction rate at constant extent of conversion is only a function of the temperature.

$$\left[\frac{d\ln(d\alpha/dt)}{dt}\right]_{\alpha} = -\frac{E_{\alpha}}{R} \tag{8}$$

(henceforth the subscript α indicates the values related to a given extent of conversion). E_α is computed for various α values ranging between 0 and 1. For single step reactions E_α is constant over the whole temperature (or conversion) interval. For multi-step kinetics, E_α will vary with α and this reflects the variation in relative contributions of single steps to the overall reaction rate. The goal of the model-free kinetics (MFK) and of the isoconversional analysis is to use this variation, as additional information on the reaction mechanism [55-62]. Common integral methods make use of various approximations to evaluate the so-called "temperature integral" [57-61]. The use of differential methods, i.e. Friedman method in the case of iso-conversional methods, avoids this limitation inherent of integral methods, but differential methods are known to be noise sensitive if no modification is used [59,61]. For these reasons, Sbirrazzuoli et al. [61] and Vyazovkin [63-64] have developed integral methods based on numerical integration. The method proposed by Sbirrazzuoli et al. [61] was called "Ozawa corrected method" while that of Vyazovkin [63-64] is the "advanced isoconversional method". An additional advantage of the advanced iso-conversional method is that it is not limited to linear temperature programs, and it takes into account possible variations in the activation energy. To estimate the E_α -dependencies for epoxy cures, we used the advanced iso-conversional method developed by Vyazovkin [63-64]. According to this method, for a set of n experiments carried out at different arbitrary heating programs $T_i(t)$, the activation energy is determined at any particular value of α by finding the value of E_α that minimizes the function

$$\sum_{i=1}^{n}\sum_{j\neq i}^{n}\frac{J\left[E_\alpha, T_i\left(t_\alpha\right)\right]}{J\left[E_\alpha, T_j\left(t_\alpha\right)\right]} \tag{9}$$

In Eq. 9 the integral

$$J\left[E_\alpha, T_i\left(t_\alpha\right)\right] \equiv \int_{t_{\alpha-\Delta\alpha}}^{t_\varepsilon} \exp\left[\frac{-E_\beta}{RT_i\left(t\right)}\right]dt \tag{10}$$

is evaluated numerically for a set of experimental heating programs. Integration is performed over small time segments (Eq.(10)) that allows for eliminating a systematic error occurring in the usual integral methods when E_α varies significantly with α. In Eq. (10), α is varied from Δα to 1− Δα with a step $\Delta\alpha = m^{-1}$, where m is the number of intervals chosen for analysis.

The eq. (9) can be further rearranged as follows:

$$\sum_{i=1}^{n}\sum_{j\neq i}^{n}\frac{I\left[E_\alpha, T_{\alpha,i}\right]\beta_j}{I\left[E_\alpha, T_{\alpha,j}\right]\beta_i} \tag{11}$$

where β is the heating rate and $I[E_\alpha, T_{\alpha,i}]$ is determined by with the help of a Doyle's approximation [65]

$$I\left(E_\alpha, T_{\alpha,i}\right) \cong \frac{E_\alpha}{R}\exp\left(-5.331-1.052\frac{E_\alpha}{RT_{\alpha,i}}\right) \tag{12}$$

The minimization procedure is repeated for each value of α to determine the E_α dependence. Iso-conversional methods determine the E_α values independent of the pre-exponential factors, which are not directly produced by these methods. This allows the elimination of the bias from the value of the activation energy which could be caused by its strong correlation with the pre-exponential factor that is generally found when both parameters are fitted simultaneously [66]. By contrast with usual iso-conversional methods, sample (non-linear) temperature variations and non-linear interpolation algorithm were used to compute the E_α -dependence, for both isothermal and non-isothermal data. The curing reaction of epoxy resin was investigated by DSC at four different heating rates (β= 2.5, 5, 10, 20 °C/min) from 30 to 300 °C; Fig. 12a shows a typical example of DSC thermograms for epoxy resin while Fig. 12b shows the variation of the fractional conversion (α) as a function of temperature for the epoxy, where

$$\alpha(T,\beta)=\frac{\Delta H_{\beta}(T)}{\Delta H_{tot}} \tag{13}$$

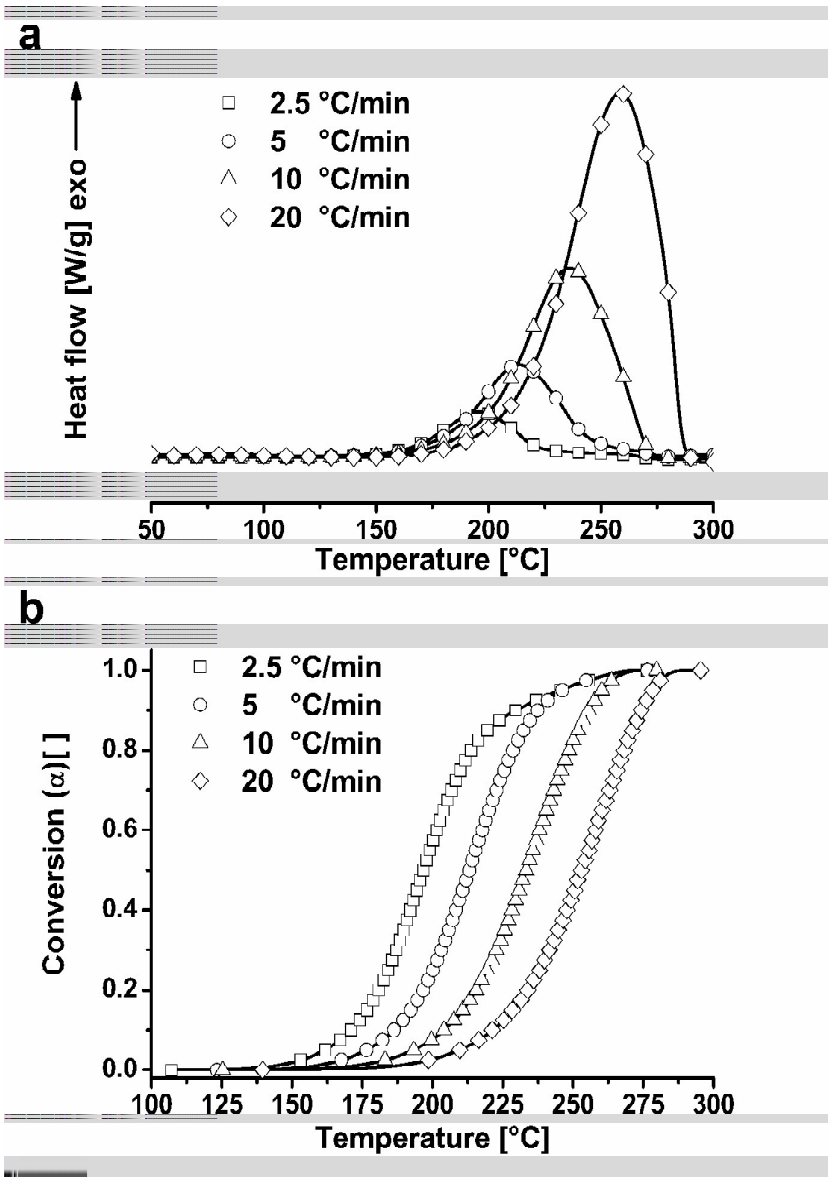

Fig. 12 A typical dynamic DSC curing curve.

The application of Eq. (11) to non-isothermal data, give rise to the dependencies of E_α on α as is shown in figure 12. The activation energy of TGMDA-DDS system increases with the increasing of the curing degree in epoxy system, and the value of activation energy ranged from 70 kJ/mol to 170 kJ/mol. The viscosity increased with the increase of the curing degree, thus more energy was required to overcome the motion among molecule chains. With the curing reaction proceeding, the curing degree increased, and the free volume only allowed local motions of the chain segments. Therefore, a great degree of cooperatives among the chain segments were required to initiate translational motion

of the segments. This would results in a large energy barrier of the segment motion, which was reflected through activation energy at later curing stages.

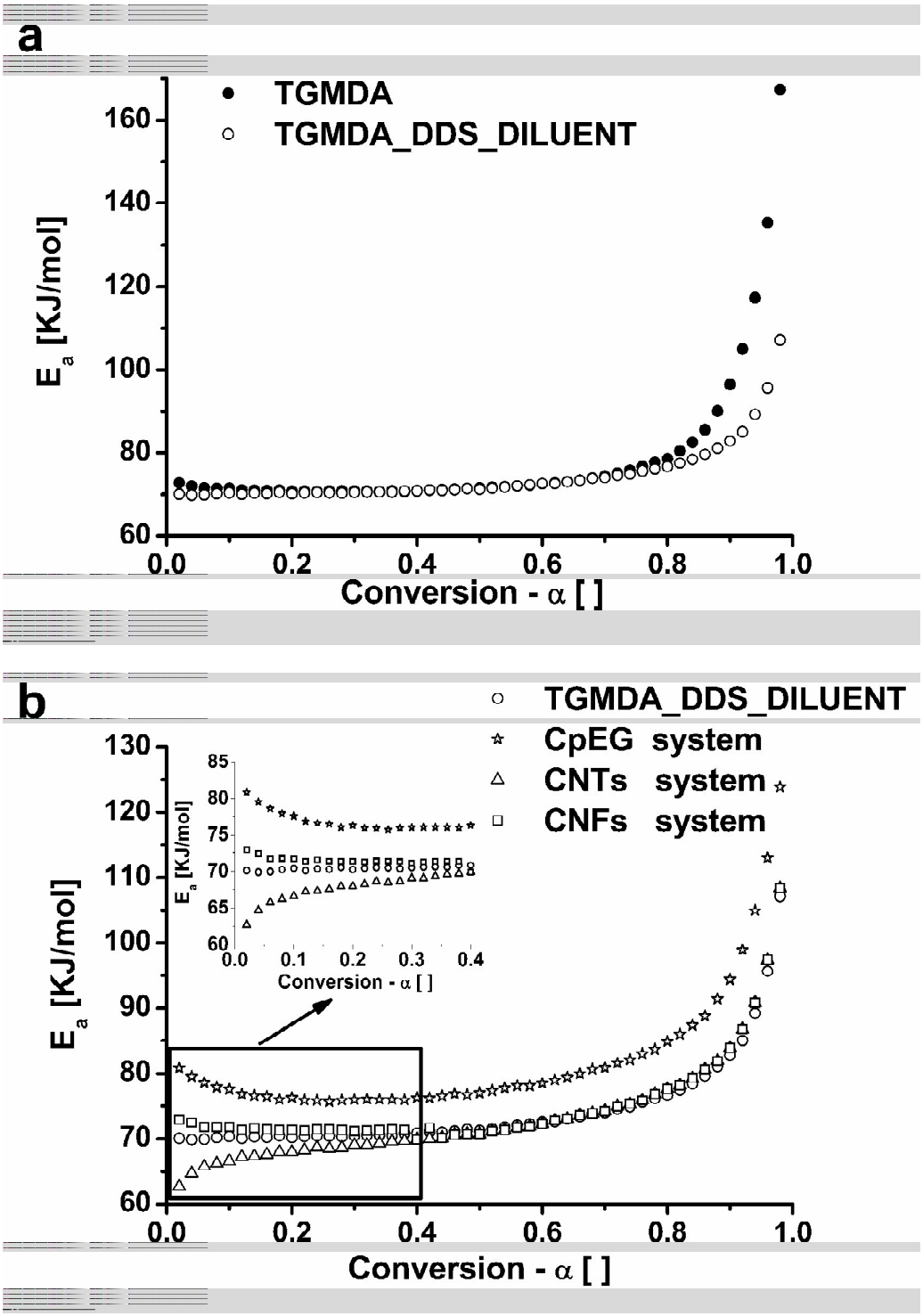

Fig. 13 Variation of the activation energy with conversion obtained for all sample.

Fig. 13a shows that the activation energy remains substantially the same for conversions under $\alpha = 0.7$ for both systems, TGMDA_DDS and TGMDA_DDS_DILUENT. For $\alpha > 0.7$ E_a is lower for the system containing the diluent. In previous studies [15], Rosu et al. have found that the presence of the reactive diluent leads to an increase of the cure range and decrease of E_a. This behaviour can be related to more comprehensive cure to the decrease of the viscosity. The decrease of the viscosity, obtained by the introduction of reactive diluent, allows the upper local motions of the chain segments. This would results in a smaller energy barrier of the segment motion, which is reflected on activation energy at later curing stages, in fact the isothermal analysis shows that the introduction of the diluent decreases particularly the activation energy of secondary amine-epoxy reaction. An additional confirmation of this effect was obtained by the dynamic DSC analysis that shows a decrease of the activation energy due to the introduction of reactive diluent, for $\alpha > 0.7$. This value is in the range of conversions (0.6-0.8) [67] in which it is considered that the reaction of secondary amine is active. The dynamic DSC analysis (see Fig 13b) shows that the behavior of one-dimensional fillers is similar to the raw resin for $\alpha > 0.4$. The effects of viscosity due to the increase of the curing degree seem to remain unaffected by the presence of the filler . The reason for this is probably due to the low concentration by weight of the filler. For $\alpha < 0.4$, in the early curing stage, the activation energy for CNT-composite slightly decreases, while for CNF-composite, the behavior is similar to the raw resin. In the literature, different works were dedicated to the determination of the effect of CNT on the curing kinetics of an epoxy resin. Xie et al. [19] also reported an acceleration effect in the case of multi-wall carbon nanotubes (MWCNT) for the TGDDM/DDS epoxy system using isothermal DSC. The higher initial reaction rate of the composites compared to the unfilled resin, the decrease of the time at maximum reaction rate and of the activation energy with increasing MWCNT content were the indication of the acceleration effect. Evidence of the presence of hydroxyl groups (–OH) on the surface of the MWCNT by FTIR spectroscopy which have a catalytic effect on epoxy ring opening was in that case the source of the modified cure. The last stage of the cure remained unaffected by MWCNT. The same group studied the effect of carbon nanofibers (CNF) on the cure behaviour of the same epoxy system [20]. They found a very small acceleration effect of CNF in the early stage of the reaction suggested by the decrease of the activation energy with an increase of the CNF content. On the other hand, the CNF hinders the reaction after that step. The origin of the acceleration effect cannot be clearly determined in their work due to the absence of surface characterization of the CNT material. The high percentage of catalyst particles in the CNT raw material may be a plausible source of the early cure initiation. In these investigations [18-20], it is believed that the modification of the cure behaviour in its early stage can be attributed to surface functional groups on CNT or catalyst particles. Wu et al. [68] studied the effect of three different carbon fillers (carbon fiber, carbon nanofiber and carbon black) on the cure reaction of the DGEBF/TETA epoxy system. They reported an increase of the total heat of reaction and a decrease of the temperature at the heat flow peak for all fillers. By comparing the effect of different

pre-treatments of the carbon fibers, they explained the increase in the total heat of reaction as a result of the presence of surface functional groups on the fillers. The authors found that the acceleration effect, that is the decrease of the peak temperature, was closely related to the specific surface area (SSA) of the filler, in view of the proportionality between the SSA and the peak temperature drop (the higher the SSA, the higher the temperature drop). In the case of this last paper, the fillers were manually dispersed in the resin and the filler content was high (around 20 wt%). The authors did not give indication on the dispersion state of the fillers; it is likely that, for this concentration of nanofillers, strong heterogeneity due to nanofiller aggregates were formed.

In our case CNT and CNF do not have any functional group, but both have small residual metal oxides. This probably explains the effect of the small decrease of the activation energy obtained in the initial stage in the CNT-composite. However the CNFs do not have effect on E_a, most likely, because the metal oxides are distributed around over a smaller surface area (Average specific surface area = 65-75 m^2g^{-1})[69] with respect to CNTs (250-300 m^2g^{-1}) [40]. In fact the CNF is an unidimensional filler as CNT, but it is characterized by a different aspect ratio length/ diameter.

In fact, the length of CNT is into a range from 0.1 to 10 μm with an average diameter of 10 nm; the length of CNF is into a range from 50 to 100 μm and a diameter into a range from 125 to 150 nm. The catalytic effect is greater if the specific surface area is higher [68]. Jana and Zhong [23] found that expanded graphite (EG) did not significantly impede the cure reaction of epoxy. Guo et al. [70] reported that at lower concentrations (1 phr) of EG, compared with the curing activation energy (E_a) of the neat epoxy resin, the composite with EG had a lower E_a before the gelation and a higher E_a after the gelation. At higher concentrations of EG (5 phr), however, in the whole conversion range, the composite with EG showed a higher E_a compared with the neat epoxy resin. In particular Jana and Zhong [23], observe that the graphite particles were comparatively heavier than epoxy resin molecules, therefore these particles could be seen as obstacles to free movement of molecules. In addition, with more conversion of the pure epoxy the viscosity of the GP/epoxy system increased and movement of epoxy molecules decreased. To initiate a translational motion of epoxy molecules, a great degree of cooperation between molecules was needed. This cooperation between epoxy molecules generated an additional amount of energy barrier to the motion of molecules and a higher amount of activation energy was needed for the conversion. Data here shown on dynamic analysis (see Fig. 13) evidence that the exfoliated graphite is characterized by an activation energy higher than the raw resin in the entire conversion range; and isothermal analysis (see Table 1) highlights that the value of E_1 and E_2 are similar for all the analyzed nanofillers, except for the value E_2 obtained for the exfoliated graphite composite. For this last filler, an increase of ~ 44 % in E_2 was detected with respect to the reference sample (TGMDA_DDS_DILUENT). Furthermore, an increase with respect to the other nanofiller (MWCNTs and CNFs) is also observed. The behaviour of the sample filled with graphite-based nanoparticles is in agreement with the general trend observed by other authors for a higher concentration of the filler and different approaches based on constant and variable activation energy to

analyse the DSC curves [23]. It is worth noting that an effective comparison is not possible due to the different approaches used in the experimental tests and the different procedure of graphite preparation. However, a such increase in the E_2 for a low amount of CpEG seems effectively relevant. This unexpected relevant increase is very likely due to self-assembly structure generated by edge-carboxylated layers inside the epoxy matrix. This architecture, on the one hand is able to enhance the electrical percolation paths and mechanical performance; on the other hand constitutes a sort of rigid nano-cages where the curing reactions must be active under condition of reduced mobility for the segmental parts of the resins. This hypothesis is confirmed by the following observation: only the E_2 value is higher than the values of E_2 related to other mono-dimensional nanofiller. Furthermore, a slight decrease is observed in E_1 value with respect to the samples loaded with MWCNTs and CNFs. This is exactly the expected result, if we consider that the functional groups on the graphene edges contributes to facilitate the curing reactions. In fact, the expected result for E_1 value is a general increase due to the physical impediment caused by the nanofillers to the network formation in the domains of the resin. This is in agreement with the observed values for CNTs and CNFs, while a value similar to the reference sample (TGMDA_DDS_DILUENT) is observed for CpEG sample.

In literature, graphene and exfoliated graphite used to impart functional properties or simply as reinforcement for the polymer, were produced using different procedure and then different structure, functionalizations and morphological features. For this reason, it is really necessary an accurate characterization of the nanofiller to understand the correlations between structural and morphological organization of graphene-based materials and curing kinetics of the nanofilled formulations. The measurements carried out in this paper employed a nanofiller exhaustively characterized in a previous manuscript [30]. In particular, in this paper a sample of exfoliated graphite able to enhance electrical and mechanical properties of the resin was used (see section 3.1).

It is very likely that the increase of the activation energy, in the exfoliated graphite composite, is determined by the same mechanisms responsible of the beneficial effects on other properties such as electrical and mechanical properties [30].

4. Conclusion

In this work, the curing kinetic reaction of a carbon/epoxy nanocomposites based systems was investigated by DSC. The dynamic experiments show that the presence of the reactive diluent leads to a decrease of the activation energy for $\alpha > 0.7$ for which it is considered that the reaction of secondary amine is active. Under the isothermal condition, the Kamal's diffusion controlled model confirm this effect, in fact the activation energies E_1 and E_2 decreased significantly, compared to the system without the reactive diluent, in particular E_2 decreases by about approximately 50%, compared to the value obtained with the system TGMDA-DDS. The effect of the nanofillers in the

TGMDA_DDS_Diluent system was analysed. The inclusion in the resin of one-dimensional fillers does not lead to big differences in the curing kinetics behaviour with respect to the unfilled epoxy mixture (TGMDA_DDS_DILUENT). Conversely, an increase in the activation energy E_2 related to secondary amine-epoxy reaction is found in the case of highly exfoliated graphite even for a very low percentage of filler (0.5 % by wt).

This increase is very likely due to self-assembly structure generated by the edge-carboxylated layers of graphite nanoparticles inside the epoxy matrix. This architecture constitutes a sort of rigid nano-cages where the final curing reactions must be active under condition of more reduced mobility with respect to the conditions experimented by other mono-dimensional nanofillers. This hypothesis seems to be confirmed by the higher value of E_2 and the slight decrease in E_1 value observed for the nanocomposites loaded with graphite-based nanoparticles with respect to other mono-dimensional nanofillers.

Acknowledgements

The research leading to these results has received funding from the European Union's Seventh Framework Programme for research, technological development and demonstration under Grant Agreement no. 313978.

References

[1] B.Z. Jang, *Advanced polymer composites: principles and applications*, ASM International, Materials Park, OH 44073-0002, USA, 1994, 305.

[2] J.K. Kim and Y.W. Mai, *Engineered interfaces in fiber reinforced composites*, Elsevier, The Boulevard, Langford Lane Kidlington, Oxford OX5 1GB, U.K, 1998, ISBN 0-08-042695-6 (hardcover).

[3] E. Mäder, Study of fibre surface treatments for control of interphase properties in composites, *Composites Science and Technology*, 1997, **57**, 1077-1088. DOI:10.1016/S0266-3538(97)00002-X

[4] W. Jia, R. Tchoudakov, R. Joseph, M. Narkis and A. Siegmann, The conductivity behavior of multi component epoxy, metal particle, carbon black, carbon fibril composites, *Journal of Applied Polymer Science*, 2002, **85**, 1706-1713. DOI: 10.1002/app.10808

[5] J. Mijović and H.T. Wang, Cure kinetics of neat and graphite-fiber-reinforced epoxy formulations, *Journal of Applied Polymer Science*, 1989, **37**, 2661-2673. DOI: 10.1002/app.1989.070370917

[6] T. Kawaguchi and R.A. Pearson, The effect of particle–matrix adhesion on the mechanical behavior of glass filled epoxies: Part 1. A study on yield behavior and cohesive strength, *Polymer*, 2003, **44**, 4229-4238. DOI:10.1016/S0032-3861(03)00371-9

[7] T. Iijima, S. Miura, W. Fukuda and M. Tomoi, Effect of cross-link density on modification of epoxy resins by N-phenylmaleimide-styrene copolymers, *European Polymer Journal*, 1993, **29**, 1103-1113. DOI:10.1016/0014-3057(93)90317-9

[8] U.M. Vakil and G.C. Martin, Crosslinked epoxies: Network structure characterization and physical–mechanical properties, *Journal of Applied Polymer Science*, 1992, **46**, 2089-2099. DOI: 10.1002/app.1992.070461204

[9] M.E. Frigione, L. Mascia and D. Acierno, Oligomeric and polymeric modifiers for toughening of epoxy resins, *European Polymer Journal*, 1995, **31**, 1021-1029.
DOI:10.1016/0014-3057(95)00091-7

[10] Y.-g. Won, J. Galy, J.F. Gérard, J.P. Pascault, V. Bellenger and J. Verdu, Internal antiplasticization in copolymer and terpolymer networks based on diepoxides, diamines and monoamines, *Polymer*, 1990, **31**, 1787-1792.
DOI:10.1016/0032-3861(90)90203-B

[11] J.R. Thakkar, R.D. Patel, R.G. Patel and V.S. Patel, Glass fibre reinforced composites of triglycidyl-p Aminophenol, *British Polymer Journal*, 1990, **22**, 143-146.
DOI: 10.1002/pi.4980220208

[12] F. Mustata, I. Bicu and C. Cascaval, Rheological and thermal behaviour of an epoxy resin modified with reactive diluents, *Journal of polymer engineering*, 1997, **17**, 491-506.
DOI: 10.1515/POLYENG.1997.17.6.491

[13] K.S. Jagadeesh, J. Gururaja Rao, K. Shashikiran, S. Suvarna, S.Y. Ambekar, M. Saletore, C. Biswas and A.V. Rajanna, Cure kinetics of multifunctional epoxies with 2,2′-dichloro-4,4′-diaminodiphenylmethane as hardener, *Journal of Applied Polymer Science*, 2010, **77**, 2097-2103.
DOI: 10.1002/1097-4628(20000906)77:10<2097::AID-APP1>3.0.CO;2-4

[14] N. Sbirrazzuoli, S. Vyazovkin, A. Mititelu, C. Sladic and L. Vincent, A Study of Epoxy-Amine Cure Kinetics by Combining Isoconversional Analysis with Temperature Modulated DSC and Dynamic Rheometry, *Macromolecular Chemistry and Physics*, 2003, **204**, 1815-1821.
DOI: 10.1002/macp.200350051

[15] D. Roşu, C.N. Caşcaval, F. Mustaţă and C. Ciobanu, Cure kinetics of epoxy resins studied by non-isothermal DSC data, *Thermochimica Acta*, 2002, **383**, 119-127.
DOI:10.1016/S0040-6031(01)00672-4

[16] A. Catalani and M.G. Bonicelli, Kinetics of the curing reaction of a diglycidyl ether of bisphenol A with a modified polyamine, *Thermochimica Acta*, 2005, **438**, 126-129.
DOI:10.1016/j.tca.2005.07.017

[17] L. Yao, J. Deng, B. J. Qu and W.F. Shi, Cure Kinetics of DGEBA with Hyperbranched Poly(3-hydroxyphenyl) Phosphate as Curing Agent Studied by Non-isothermal DSC, *Chemical Research in Chinese Universities*, 2006, **22**, 118-122.
doi:10.1016/S1005-9040(06)60059-7

[18] D. Puglia, L. Valentini, I. Armentano and J. M. Kenny, Effects of single-walled carbon nanotube incorporation on the cure reaction of epoxy resin and its detection by Raman spectroscopy, *Diamond and Related Materials*, 2003, **12**, 827-832.
DOI:10.1016/S0925-9635(02)00358-8

[19] H. Xie, B. Liu, Z. Yuan, J. Shen and R. Cheng, Cure kinetics of carbon nanotube/tetrafunctional epoxy nanocomposites by isothermal differential scanning calorimetry, *Journal of Polymer Science Part B: Polymer Physics*, 2004, **42**, 3701-3712.
DOI: 10.1002/polb.20220

[20] H. Xie, B. Liu, Q. Sun, Z. Yuan, J. Shen and R. Cheng, Cure kinetic study of carbon nanofibers/epoxy composites by isothermal DSC, *Journal of Applied Polymer Science*, 2005, **96**, 329-335.
DOI: 10.1002/app.21415

[21] J. Bae, J. Jang and S.-H. Yoon, Cure Behavior of the Liquid-Crystalline Epoxy/Carbon Nanotube System and the Effect of Surface Treatment of Carbon Fillers on Cure Reaction, *Macromolecular Chemistry and Physics*, 2002, **203**, 2196-2204.
DOI: 10.1002/1521-3935(200211)203:15<2196::AID-MACP2196>3.0.CO;2-U

[22] A.T. Seyhan, Z. Sun, J. Deitzel, M. Tanoglu and D. Heider, Cure kinetics of vapor grown carbon nanofiber (VGCNF) modified epoxy resin suspensions and fracture toughness of their resulting nanocomposites, *Materials Chemistry and Physics*, 2009, **118**, 234-242.
DOI:10.1016/j.matchemphys.2009.07.045

[23] S. Jana and W. H. Zhong, Curing characteristics of an epoxy resin in the presence of ball-milled graphite particles, *J Mater Sci*, 2009, **44**, 1987-1997.
DOI: 10.1007/s10853-009-3293-2

[24] A. Gupta, M. Cizmecioglu, D. Coulter, R.H. Liang, A. Yavrouian, F.D. Tsay and J. Moacanin, The mechanism of cure of tetraglycidyl diaminodiphenyl methane with diaminodiphenyl sulfone, *Journal of Applied Polymer Science*, 1983, **28**, 1011-1024.
DOI: 10.1002/app.1983.070280309

[25] J. Mijović, J. Kim and J. Slaby, Cure kinetics of epoxy formulations of the type used in advanced composites, *Journal of Applied Polymer Science*, 1984, **29**, 1449-1462.
DOI: 10.1002/app.1984.070290437

[26] L. Chiao, Mechanistic reaction kinetics of 4,4'-diaminodiphenyl, sulfone cured tetraglycidyl-4,4'-diaminodiphenylmethane epoxy resins, *Macromolecules*, 1990, **23**, 1286-1290.
DOI: 10.1021/ma00207a010

[27] C.C. Su and E.M. Woo, Diffusion-controlled reaction mechanisms during cure in polycarbonate-modified epoxy networks, *Journal of Polymer Science Part B: Polymer Physics*, 1997, **35**, 2141-2150.
DOI: 10.1002/(SICI)1099-0488(19970930)35:13<2141::AID-POLB14>3.0.CO;2-4

[28] M. Opalički, J.M. Kenny and L. Nicolais, Cure kinetics of neat and carbon-fiber-reinforced TGDDM/DDS epoxy systems, *Journal of Applied Polymer Science*, 1996, **61**, 1025-1037.
DOI: 10.1002/(SICI)1097-4628(19960808)61:6<1025::AID-APP17>3.0.CO;2-V

[29] L. Guadagno, M. Raimondo, V. Vittoria, L. Vertuccio, C. Naddeo, S. Russo, B. De Vivo, P. Lamberti, G. Spinelli and V. Tucci, Development of epoxy mixtures for application in aeronautics and aerospace, *RSC Advances*, 2014, **4**, 15474-15488.
DOI: 10.1039/C3RA48031C

[30] L. Guadagno, M. Raimondo, L. Vertuccio, M. Mauro, G. Guerra, K. Lafdi, B. De Vivo, P. Lamberti, G. Spinelli and V. Tucci, Optimization of graphene-based materials outperforming host epoxy matrices, *RSC Advances*, 2015, **5**, 36969-36978.
DOI: 10.1039/c5ra04558d

[31] U. Vietri, L. Guadagno, M. Raimondo, L. Vertuccio, K. Lafdi, Nanofilled epoxy adhesive for structural aeronautic materials, *Composites Part B: Engineering*, 2015, 61, 73-83.
DOI: 10.1016/j.compositesb.2014.01.032

[32] L. Guadagno, M. Raimondo, V. Vittoria, L. Vertuccio, K. Lafdi, B. De Vivo, P. Lamberti, G. Spinelli and V. Tucci, The role of carbon nanofiber defects on the electrical and mechanical properties of CNF-based resins, *Nanotechnology*, 2013, 24, 305704, 305704 (10 pp).
DOI: 10.1088/0957-4484/24/30/305704

[33] M. Raimondo, S. Russo, L. Guadagno, P. Longo, S. Chirico, A. Mariconda, L. Bonnaud, O. Murariu and Ph Dubois, Effect of incorporation of POSS compounds and phosphorous hardeners on thermal and fire resistance of nanofilled aeronautic resins, *RSC Advances*, 2015, **5**, 10974-10986.
DOI: 10.1039/c4ra11537f

[34] L. Guadagno, M. Raimondo, U. Vietri, L. Vertuccio, G. Barra, B. De Vivo, P. Lamberti, G. Spinelli, V. Tucci, R. Volponi, G. Cosentino and F. De Nicola, Effective formulation and processing of nanofilled carbon fiber reinforced composites, *RSC Advances*, 2015, **5**, 6033-6042.
DOI: 10.1039/C4RA12156B

[35] L. Guadagno, U. Vietri, M. Raimondo, L. Vertuccio, G. Barra, B. De Vivo, P. Lamberti, G. Spinelli, V. Tucci, F. De Nicola, R. Volponi and S. Russo, Correlation between electrical conductivity and manufacturing processes of nanofilled Carbon Fiber Reinforced Composites, *Composites Part B: Engineering*, 2015, **80**, 7-14.
doi:10.1016/j.compositesb.2015.05.025

[36] L. Guadagno, M. Sarno, U. Vietri, M. Raimondo, C. Cirillo and P. Ciambelli, Graphene-based structural adhesive to enhance adhesion performance, *RSC Advances*, 2015, **5**, 27874-27886.
DOI: 10.1039/C5RA00819K

[37] M. R. Nobile, M. Raimondo, K. Lafdi, A. Fierro, S. Rosolia and L. Guadagno, Relationships between nanofiller morphology and viscoelastic properties in CNF/epoxy resins, *Polymer Composites*, 2015, **36**, 1152–1160.
DOI: 10.1002/pc.23362

[38] L. Guadagno, M. Raimondo, K. Lafdi, A. Fierro, S. Rosolia and M. R. Nobile, Infuence of nanofiller morphology on the viscoelastic properties of CNF/epoxy resins, *AIP Conf. Proc.*, 2014, **1599**, 386-389.
DOI: 10.1063/1.4876859

[39] L. Guadagno, L. Vertuccio, A. Sorrentino, M. Raimondo, C. Naddeo, V. Vittoria, G. Iannuzzo, E. Calvi and S. Russo, Mechanical and barrier properties of epoxy resin filled with multi-walled carbon nanotubes, *Carbon*, 2009, **47**, 2419-2430.
DOI: http://dx.doi.org/10.1016/j.carbon.2009.04.035
[40] L. Guadagno, B. De Vivo, A. Di Bartolomeo, P. Lamberti, A. Sorrentino, V. Tucci, L. Vertuccio and V. Vittoria, Effect of functionalization on the thermo-mechanical and electrical behavior of multi-wall carbon nanotube/epoxy composites, *Carbon*, 2011, **49**, 1919-1930.
DOI: http://dx.doi.org/10.1016/j.carbon.2011.01.017
[41] Verônica M.A. Calado and S. G. Advani, Thermoset Resin Cure Kinetics and Rheology, *Processing of Composites*, Publisher: Carl Hanser Verlag GmbH & Co. KG, 2000, pp. 32-107.
[42] H. J. Flammersheim and J.R. Opfermann, Kinetic evaluation of DSC curves for reacting systems with variable stoichiometric compositions, *Thermochimica Acta*, 2002, **388**, 389-400.
DOI: http://dx.doi.org/10.1016/S0040-6031(02)00042-4
[43] A.A. Skordos and I.K. Partridge, Cure kinetics modeling of epoxy resins using a non-parametric numerical procedure, *Polymer Engineering & Science*, 2001, **41**, 793-805.
DOI: 10.1002/pen.10777
[44] Y. Hou-Yong, Q. Zong-Yi, S. Bin, Y. Xiao-Gang, Y. Ju-Ming, Reinforcement of transparent poly(3-hydroxybutyrate-co-3-hydroxyvalerate) by incorporation of functionalized carbon nanotubes as a novel bionanocomposite for food packaging, *Composites Science and Technology*, 2014, **94**, 96–104.
DOI:10.1016/j.compscitech.2014.01.018
[45] K. Hun-Sik, P. Byung Hyun, Y. Jin-San, J. Hyoung-Joon, Thermal and electrical properties of poly(L-lactide)-graft-multiwalled carbon nanotube composites, *European Polymer Journal* 2007, **43,** 1729–1735
DOI:10.1016/j.eurpolymj.2007.02.025
[46] M.R. Keenan, Autocatalytic cure kinetics from DSC measurements: Zero initial cure rate, *Journal of Applied Polymer Science*, 1987, **33**, 1725-1734.
DOI: 10.1002/app.1987.070330525
[47] C.C. Su and E.M. Woo, Cure kinetics and morphology of amine-cured tetraglycidyl-4,4′-diaminodiphenylmethane epoxy blends with poly(ether imide), *Polymer*, 1995, **36**, 2883-2894.
DOI: http://dx.doi.org/10.1016/0032-3861(95)94337-S
[48] G. Jungang, L. Deling, S. Shigang and L. Guodong, Curing kinetics and thermal property characterization of a bisphenol-F epoxy resin and DDO system, *Journal of Applied Polymer Science*, 2002, **83**, 1586-1595.
DOI: 10.1002/app.10139
[49] E. Rabinowitch, Collision, co-ordination, diffusion and reaction velocity in condensed systems, *Transactions of the Faraday Society*, 1937, **33**, 1225-1233.
DOI: 10.1039/TF9373301225
[50] G. Wisanrakkit and J.K. Gillham, The glass transition temperature (Tg) as an index of chemical conversion for a high-Tg amine/epoxy system: Chemical and diffusion-controlled reaction kinetics, *Journal of Applied Polymer Science*, 1990, **41**, 2885-2929.
DOI: 10.1002/app.1990.070411129
[51] S.L. Simon and J.K. Gillham, Cure kinetics of a thermosetting liquid dicyanate ester monomer/high-Tg polycyanurate material, *Journal of Applied Polymer Science*, 1993, **47**, 461-485.
DOI: 10.1002/app.1993.070470308
[52] J. Fournier, G. Williams, C. Duch and G.A. Aldridge, Changes in Molecular Dynamics during Bulk Polymerization of an Epoxide−Amine System As Studied by Dielectric Relaxation Spectroscopy, *Macromolecules*, 1996, **29**, 7097-7107.
DOI: 10.1021/ma9517862
[53] C.S. Chern and G.W. Poehlein, A kinetic model for curing reactions of epoxides with amines, *Polymer Engineering & Science*, 1987, **27**, 788-795.
DOI: 10.1002/pen.760271104
[54] D. Ratna, *Handbook of thermoset resins*, Publisher: Smithers Rapra Technology, Shawbury, UK, 2009.
[55] S. Du, Z. S. Guo, B. Zhang and Z. Wu, Cure kinetics of epoxy resin used for advanced composites, *Polymer International*, 2004, **53**, 1343-1347.

DOI: 10.1002/pi.1533
[56] V.L. Zvetkov. Comparative DSC kinetics of the reaction of DGEBA with aromatic diamines.: I. Non-isothermal kinetic study of the reaction of DGEBA with m-phenylene diamine, *Polymer*, 2001, **42**, 6687-6697.
DOI: http://dx.doi.org/10.1016/S0032-3861(01)00160-4
[57] E. Turi, *Thermal characterization of polymeric materials*, Elsevier, 2012.
[58] S. Vyazovkin and N. Sbirrazzuoli, Kinetic methods to study isothermal and nonisothermal epoxy-anhydride cure, *Macromolecular Chemistry and Physics*, 1999, **200**, 2294-2303.
DOI: 10.1002/(SICI)1521-3935(19991001)200:10<2294::AID-MACP2294>3.0.CO;2-V
[59] S. Vyazovkin and N. Sbirrazzuoli, Mechanism and Kinetics of Epoxy-Amine Cure Studied by Differential Scanning Calorimetry, *Macromolecules*, 1996, **29**, 1867-1873.
DOI: 10.1021/ma951162w
[60] S. Vyazovkin and N. Sbirrazzuoli, Isoconversional method to explore the mechanism and kinetics of multi-step epoxy cures, *Macromolecular Rapid Communications*, 1999, **20**, 387-389.
DOI: 10.1002/(SICI)1521-3927(19990701)20:7<387::AID-MARC387>3.0.CO;2-S
[61] N. Sbirrazzuoli, Y. Girault and L. Elégant, Simulations for evaluation of kinetic methods in differential scanning calorimetry. Part 3—Peak maximum evolution methods and isoconversional methods, *Thermochimica Acta*, 1997, **293**, 25-37.
DOI: http://dx.doi.org/10.1016/S0040-6031(97)00023-3
[62] N. Sbirrazzuoli, S. Vyazovkin, A. Mititelu, C. Sladic and L. Vincent, A Study of Epoxy-Amine Cure Kinetics by Combining Isoconversional Analysis with Temperature Modulated DSC and Dynamic Rheometry, *Macromolecular Chemistry and Physics*, 2003, **204**, 1815-1821.
DOI: 10.1002/macp.200350051
[63] S. Vyazovkin, Evaluation of activation energy of thermally stimulated solid-state reactions under arbitrary variation of temperature, *Journal of Computational Chemistry*, 1997, **18**, 393-402.
DOI: 10.1002/(SICI)1096-987X(199702)18:3<393::AID-JCC9>3.0.CO;2-P
[64] S. Vyazovkin, Modification of the integral isoconversional method to account for variation in the activation energy, *Journal of Computational Chemistry*, 2001, **22**, 178-183.
DOI: 10.1002/1096-987X(20010130)22:2<178::AID-JCC5>3.0.CO;2-#
[65] C.D. Doyle, Estimating isothermal life from thermogravimetric data, *Journal of Applied Polymer Science*, 1962, **6**, 639-642.
DOI: 10.1002/app.1962.070062406
[66] N. Sbirrazzuoli, L Vincent and S. Vyazovkin, Comparison of several computational procedures for evaluating the kinetics of thermally stimulated condensed phase reactions, *Chemometrics and Intelligent Laboratory Systems*, 2000, **54**, 53-60.
DOI: http://dx.doi.org/10.1016/S0169-7439(00)00103-9
[67] Q. Li, X. Li and Y. Meng, Curing of DGEBA epoxy using a phenol-terminated hyperbranched curing agent: Cure kinetics, gelation, and the TTT cure diagram, *Thermochimica Acta*, 2012, **549**, 69-80.
DOI: http://dx.doi.org/10.1016/j.tca.2012.09.012
[68] J. Wu and D.D.L. Chung, Calorimetric study of the effect of carbon fillers on the curing of epoxy, *Carbon*, 2004, **42**, 3039-3042.
DOI: http://dx.doi.org/10.1016/j.carbon.2004.07.010
[69] B. De Vivo, P. Lamberti, G. Spinelli, V. Tucci, L. Guadagno, M. Raimondo, The effect of filler aspect ratio on the electromagnetic properties of carbon-nanofibers reinforced composites, *Journal of Applied Physics*, 2015, **118**, 064302.
DOI: 10.1063/1.4928317
[70] B. W.J. Guo, Y. Lei, D. Jia, Curing behaviour of epoxy resin/graphite composites containing ionic liquid, *Journal of Physics D: Applied Physics*, 2009, **42**, 145307/145301–145307/145308.
DOI: 10.1088/0022-3727/42/14/145307